Atypical Lyman-α emission in a dwarf galaxy via multiphase gas and rotation.

Jaime E. Forero-Romero [1] $\star$, Max Gronke[2], María Camila Remolina-Gutiérrez[1],
Nicolás Garavito-Camargo[3], Mark Dijkstra[2]

[1] *Departamento de Física, Universidad de los Andes, Cra. 1 No. 18A-10 Edificio Ip, CP 111711, Bogotá, Colombia*
[2] *Institute of Theoretical Astrophysics, University of Oslo, Postboks 1029 Blindern, NO-0315 Oslo, Norway.*
[3] *Department of Astronomy, University of Arizona, 933 North Cherry Avenue, Tucson, AZ 85721, USA.*

16 January 2017

ABSTRACT
Star-forming Compact Dwarf Galaxies (CDGs) resemble the expected pristine conditions of the first galaxies in the Universe. Before the observational detection of the first galaxies becomes reality, CDGs are the best systems to test our ideas on primordial galaxy formation and evolution. Here we report on one of such CDGs, Tololo 1214-277, which presents a broad symmetric Lyman-α line emission that had evaded theoretical interpretation so far. In this letter we explain these features by two different models: an homogeneous gaseous sphere undergoing bulk rotation and an interstellar medium composed by outflowing clumps with additional random motions. It is the first time that an observed Lyα spectrum can be explained assuming either of these physical conditions. We find that both models independently require high velocities (either a bulk rotation of 348^{+75}_{-48} km s^{-1} or a clump velocity dispersion of 54.3 ± 0.6 km s^{-1} with outflows of 54.3 ± 5.1 km s^{-1}) consistent with a dynamical mass of at least a billion solar masses, ten times larger than its baryonic mass. We argue that a possible explanation for this excess of dynamical mass is the presence of a supermassive black hole at the center of Tololo 1214-277. This work demonstrates the importance of considering multiphase physics and rotation among the possible conditions shaping the Lyα spectra of the first galaxies. Additionally, if future kinematic maps of Tololo 1214-277 confirm the high velocities postulated in our model, it would provide new evidence for dwarf galaxies as hosts of supermassive black holes.

Key words: Methods: data analysis - numerical

1 INTRODUCTION

The first generation of galaxies trace our cosmic origins. They were the first steps in the evolution of galaxies such as the Milky Way. In the standard Big Bang cosmology the only chemical elements that were created in the nucleosynthesis process were Hydrogen, Helium and Lithium. Heavier elements must have been created in stellar evolution process. Therefore, we expect the first generation of galaxies to be metal free and rich in Hydrogen. This kind of primordial galaxies have not been detected yet. However, dwarf star forming galaxies with a low metallicity content are seen as templates to understand the early galaxy evolution process.

Almost fifty years ago (Partridge & Peebles 1967) it was realized that young galaxies could be detected through a strong Lyman-α line emission.

This theoretical prediction was only confirmed thirty years later on distant, relatively young, not primordial, galaxies (Dey et al. 1998). Currently Lyman Alpha Emitting (LAE) galaxies are commonly targeted in surveys. The presence of the Ly-α emission line provides confirmation of the distance of a galaxy while provides clues about the stellar population and inter-stellar medium conditions regulating the Ly-α emission.

The Ly-α emission line is not exclusive of distant galaxies. Any galaxy with low dust content and ongoing star formation has the right conditions to show this line. There are, for instance, local Universe surveys that target Ly-α emission in nearby dwarf star forming galaxies (Östlin et al. 2014). The study of nearby LAE samples has allowed the study of other indicators that might be more difficult to obtain for distant galaxies such as morphology, dust attenuation, neutral hydrogen contents and ionization state.

However, the physical interpretation of Ly-α observa-

$\star$ je.forero@uniandes.edu.co

tions is not straightforward (Rivera-Thorsen et al. 2015). This is due to the resonant nature of the Ly-α line. A Ly-α photon follows a diffusion-like process before escaping the galaxy or being absorbed by dust. The resulting line profile becomes sensitive to the dynamical, chemical and thermal conditions in the interstellar medium. There are very few analytically tools available to interpret the emerging Ly-α line. They are applicable only in very few cases of highly symmetrical conditions, which are hardly met in real astrophysical systems. For these reasons the interpretation of Ly-α observations requires state-of-the-art Monte Carlo radiative transfer simulations.

Tololo 1214-277 is a compact star forming dwarf galaxy that presents a strong Ly-α emission (Thuan & Izotov 1997) with two puzzling features: the line is symmetric and single peaked. Usually the Ly-α line has an asymmetric single or double peak. These two special features in Tololo 1214-277 cannot be explained with conventional models (Verhamme et al. 2006; Gronke et al. 2015).

In this letter we show how the Tololo 1214-277's Lyα profile can be explained either by rotation (Garavito-Camargo et al. 2014) or the recently developed class of more complex multiphase models that predict a wider variety of spectra including, single, double and triply peaked spectra (Gronke & Dijkstra 2016). Figure 1. summarizes our findings. Dots represent the observational data for Tololo 1214-277 with the overplot from our best fits from the analytical solution for a rotating homogeneous gas sphere (thin line) and the multiphase model (thick line). This is the first time that these models have been introduced with success to explain an observed Lyα profile.

The best parameters in the rotation model are a rotational velocity of $V_{\max} = 348^{+75}_{-48}$ km s^{-1}, a neutral Hydrogen optical depth of $\log_{10} \tau = 6.96^{+0.26}_{-0.18}$, and an inter-stellar medium temperature of $\log_{10} T/\mathrm{K} = 4.27^{+0.11}_{-0.18}$. This model is also able to constrain the angle between the plane perpendicular to the rotation axis and the observational line-of-sight to $\theta = 35.78^{+2.13}_{-1.88}$ degrees.

In the multiphase model the best constrained parameters by the observational data are the clump velocity dispersion $\sigma_{\mathrm{cl}} = 54.3 \pm 0.6$ km s^{-1}, the clump's outflowing velocity $v_{\infty,\mathrm{cl}} = 54.3 \pm 5.1$ km s^{-1} and the fraction of the Lyα emission that is coming from the cold clumps $P_{\mathrm{cl}} = 0.96 \pm 0.01$.

Assuming that the clumps are located in a spherical region of radius $r_s = 2.25$ kpc (corresponding to Tololo 1214-277's estimated 3D half-luminosity radius), this corresponds to dynamical masses of $M_{\mathrm{dyn}} = 3.2^{+1.6}_{-1.0} \times 10^{10} M_\odot$ and $M_{\mathrm{dyn}} = 2.31 \pm 0.04 \times 10^9 \, M_\odot$ for the rotation and multiphase models, respectively,

Tololo 1214-277's stellar mass is $M_\star = 1.45 \pm 0.45 \times 10^8 M_\odot$ (Madden et al. 2014) and its total neutral HI mass is $M_{\mathrm{HI}} < 2.65 \times 10^8 \, \mathrm{M}_\odot$ (Pustilnik & Martin 2007); the dynamical mass is at least 12 to 160 times the baryonic mass, depending if one considers the multiphase or rotation estimate.

We lean towards the lower dynamical mass estimate from the multiphase model as it seems easier to reconcile with the following two astrophysical mechanisms for its origin. The first way to explain a dynamical mass of $10^9 M_\odot$ in a sphere of 2.25 kpc in radius, could be a dark matter halo of at least $10^{12} \, \mathrm{M}_\odot$ in mass (Tollerud et al. 2011), which leaves open the question as to why Tololo 1214-277 is not

more similar to the Milky Way galaxy as it would be hosted by a dark matter halo of similar mass. A second possibility is that Tololo 1214-277 hosts a supermassive black hole of $10^9 M_\odot$. This is almost two orders of magnitude higher than the supermassive black hole found in the compact dwarf galaxy M60-UCD1 (Seth et al. 2014), which has a similar stellar mass as Tololo 1214-277. This would leave open the question about the formation process of such a system.

Another perspective to appreciate the atypically high dynamical mass estimates comes from the observed scaling relations for dwarf galaxies. Assuming that Tololo 1214-277 followed the fundamental plane relationship between its mean surface brightness I_e, the projected half-light radius R_e and the velocity dispersion σ, described by $\log I_e = 1.6 \log \sigma - 1.21 \log R_e + 0.55$ (Graves et al. 2009), the expected velocity dispersion should be on the order of 5 ± 1 km s^{-1}, which is a factor of $\sim$ 10 - 60 lower than the results from the multiphase and rotation models, respectively. These are equivalent to factors of $\sim$ 100 - 3600 on the dynamical mass. Once again, Tololo 1214-277 seems to be significantly more massive than expected.

A new observational test is needed to clarify the physical nature of Tololo 1214-277. We suggest that integral field unit measurements spatially resolving its spatial extent are up to the task. Tololo 1214-277 spans a region of 4 arcseconds, an instrument such as the Multi Unit Spectroscopic Explorer (Bacon et al. 2014) with its nominal 0.2 arcseconds spatial sampling over a 1.0 arcminute field in wide-field mode could provide a coarse mapping of different ionization lines to infer a kinematic map. Another observational test includes the measurement of the Lyα ionizing continuum escape fraction. In the rotational model this fraction should be zero, while the multiphase model predicts that averaging over all sightlines it should be around $0.5^{+1.0}_{-0.4}\%$, with the possibility of strong variations depending on viewing angle (Gronke & Dijkstra 2014).

All in all, the mere existence of a strong LAE galaxy with a broad, symmetric line is interesting. It raises the question whether some high redshift LAEs have asymmetric lines because the blue half was truncated by the intergalactic medium. In this case the Lyα radiation could emerge as a low surface brightness glow, which may be connected to Lyα halos, while also influencing the way LAEs can be used as a probe of reionization (Dijkstra 2014).

These findings demonstrate the importance of including rotation and multiphase conditions as features to model the Lyα line in high redshift galaxies. Additionally, if the hypothesis of a supermassive black hole in Tololo 1214-277 proves to be consistent with future observational kinematic maps, it could correspond to a so far undetected supermassive black hole in a dwarf galaxy, providing a new way to test and probe theories on the co-evolution of galaxies and black holes in the first generation of galaxies.

Tololo 1214-277 CHARACTERISTICS

Tololo 1214-277 receding velocity is 7785 ± 50km s^{-1}, which translates into a distance of 106.6 Mpc (with the Hubble constant H_0=73 Mpc km s^{-1}) Its metallicity is $\sim Z_\odot/24$ (Izotov et al. 2004) as derived from optical spectroscopy.

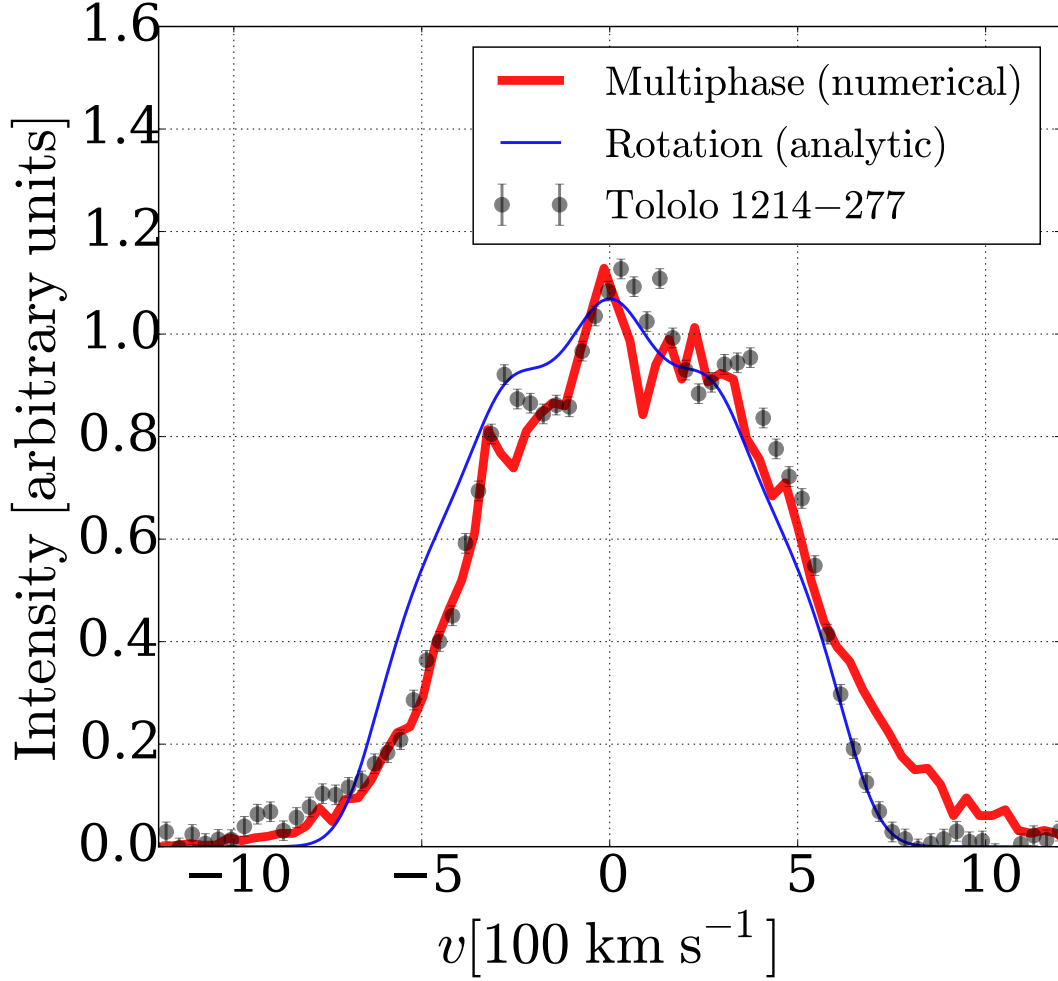The observed flux for the Lyman alpha line is $\sim 8.1 \times$

Figure 1. Broad, single peaked and symmetric Ly-α emission of Tololo 1214-277. Dots correspond to the observational data. The line shows the results of our best model from a full radiative transfer simulation both for the rotation and multiphase models.

$\alpha(2000)^a$	12h17min17.1s
$\delta(2000)^b$	-28d02m32s
l, b (deg)	294, 34
m_V	17.5
M_V	-17.6
v(km s^{-1})	7795
Ly-α (erg cm^{-2} s^{-1} Å^{-1})	8.1×10^{-14}
Ly-α EW	70Å
Hβ (erg cm^{-2} s^{-1} Å^{-1})	1.62×10^{-14}
21cm (Jy km s^{-1})	< 0.10

Table 1: Basic observational characteristics of TOL1214-277 (Thuan & Izotov 1997)

10^{-14} erg cm^{-2} s^{-1} (Thuan & Izotov 1997) and a Equivalent Width of 70Å and its Hβ flux is 1.62×10^{-14} erg cm^{-2} s^{-1} Å-1 (Izotov et al. 2004) which gives a Lyα/Hβ flux ratio of 4.9±0.1. The Ly-α flux values correspond to luminosities of $L_{Ly\alpha} = 2.2 \times 10^{42}$ erg s^{-1} over a 20Å bandwidth, which in turns translates into a star formation rate of 2.0 M$_\odot$ yr^{-1} using a standard conversion factor between luminosity and

star formation rate of 9.1×10^{-43} $L_{Ly\alpha}$ M$_\odot$ yr^{-1}. The absolute magnitude in the V band translates into a luminosity of 8.9×10^8 L$_\odot$. Comparing this ratio with the theoretical expectation from case B recombination of 23.3 (Hummer & Storey 1987) one can estimate an escape fraction of 20% for Lyα radiation. The bolometric UV luminosity is $9.43 \pm 1.94 \times 10^8$ L$_\odot$ as measured by GALEX.

There is an upper limit for the integrated flux of < 0.10 Jy km s^{-1}, which translates into a upper limit for the HI mass of $M < 2.65 \times 10^8$ M$_\odot$ (Pustilnik & Martin 2007).

The near-infrared fluxes at 3.6 μm and 4.5 μm are $7.71 \pm 0.55 \times 10^{-5}$ Jy and $7.98 \pm 0.71 \times 10^{-5}$ Jy (Engelbracht et al. 2008). Using a conversion between fluxes and stellar mass calibrated on the Large Magellanic Cloud $M_\star = 10^{5.65} \times F_{3.6}^{2.85} \times F_{4.5}^{-1.85} \times (D/0.05)^2 M_\odot$, where fluxes are in Jy and D is the luminosity distance to the source in Mpc, we find $M_\star = 1.45 \pm 0.45 \times 10^8 M_\odot$, with a 30% uncertainty coming from the calibration process (Eskew et al. 2012).

We computed the projected half-luminosity radius to be $R_s = 1.5 \pm 0.1$ kpc from the surface intensity profiles reported by. (Noeske et al. 2003). Assuming spherical geometry, one can translate this value into a 3D half-luminosity radius of $r_s = 3R_s/2 = 2.25$ kpc.

THE ROTATION MODEL

The rotation model corresponds to the work presented in (Garavito-Camargo et al. 2014) based on the Monte Carlo code CLARA (Forero-Romero et al. 2011). In that model the Ly-α photons are propagated within a spherical and homogeneous cloud of HI gas undergoing solid body rotation. The sphere is fully characterized by three parameters: the HI line's center optical depth τ measured from the center to its surface, the HI temperature T, and the linear surface velocity $V_{\max}$. Photons are emitted at their natural frequency from the center of the sphere. Including the effect of dust only changes the overall line normalization but not its shape. The results we report in the main body of the paper do not include any dust model. In this letter we use an analytical solution that captures the most important effects of rotation onto the Lyα line.

The first important effect of rotation is that it breaks the spherical symmetry of the static case. Now the line's observed morphology depends on the angle θ between the line-of-sight (LOS) and the rotation axis. LOS parallel to the rotation axis tend to observed the line without any modification from rotation, while the perpendicular LOS will observe a maximal change in the line's morphology due to rotation.

The main change in the line's morphology is that it broadens and the intensity at the center increases. For high enough rotational velocities the intensity at the peak's center increases so much that the line goes from double to single peaked, sometimes slightly triple peaked. This is the feature that allows this model to fit the observational features of Tololo 1214-277.

(Garavito-Camargo et al. 2014) derived a concise analytical description for those features. This description takes into account how different parts of the sphere's surface shift in frequency the Lyα photons. Different shifts in frequency come from different values for the projected velocity along the LOS. Using the analytical solution for the Lyα spectra of a static sphere plus the right frequency shifts computed from geometrical considerations, one is able to compute an analytical solution for the rotating sphere that reproduces the main features found using the full numerical simulation.

The analytical solution for the rotation sphere was the base to perform the Markov Chain Monte Carlo (MCMC) calculation using the emcee Python library (Foreman-Mackey et al. 2013). emcee is an open source optimized implementation of the affine-invariant ensemble sampler for MCMC. The algorithm creates a number of walkers that, during a sufficient number of steps, generate parameters' combinations for a specific model. For each time, the code calculates the likelihood of the combination with respect to the observational data. The walkers ecplore the parameter space sampling the likelihood function.

MCMC methods are optimal for sampling parameters at a high number of dimensions. In this case we explore flat priors on four parameters: $200 < V_{\max}/\text{km s}^{-1} < 600$, $6.0 < \log_{10} \tau < 9.0$, $4.0 < \log_{10} T/10^4\text{K} < 4.5$ and $0 < \theta < 90$ using 500 steps with 24 walkers for a total of 12000 points in the chain. The results are summarized in Figure 2. From this model we find that the fiducial parameters that could explain the broad features in Tololo 1214-277 are $V_{\max} = 348^{+75}_{-48}$ km s^{-1}, $\log \tau = 6.96^{+0.26}_{-0.18}$, $\log_{10} T/\text{K} = 4.27^{+0.11}_{-0.18}$ and $\theta = 35.78^{+2.13}_{-1.88}$ degrees.

THE MULTIPHASE MODEL

The idealized multiphase model consists of spherical, cold, dens clumps of neutral hydrogen (and dust) embedded in a hot, ionized medium. The clumps also have a random and an outflowing velocity component which totals the number of parameters describing the model to be 14.

In order to map out this large parameter space, we randomly drew 2500 sets of parameters within a observationally realistic range (based on the considerations of (Laursen et al. 2013)) yielding a large variety of single-, double- and triple-peaked spectra. The full analysis of the the spectral features as well as more details on the radiative transfer are presented in (Gronke & Dijkstra 2016). For the current work, we computed the χ^2 for each of the 2500 models. We selected the best 50 models with the lowest χ^2. The χ^2 gap in those 50 models is close to 3000, the lowest χ^2 is close to 1200. The total number of degrees of freedom is 104.

Then we performed a Kolmogorov-Smirnov test to compare each parameter distribution in the best 50 models against the parent distribution of 2500 models. If we obtain a p-value < 0.05 for a given parameter, we conclude that this parameter does influence the χ^2 fit, as the distribution for the best χ^2 models is statistically different to the distribution from the global sample of 2500 models.

From this test we found that only three parameters influence the χ^2: the clump outflow velocity $v_{\infty,\text{cl}}$ (p-value 10^{-18}), the clump velocity dispersion σ_{cl} (p-value 10^{-4}) and the probability that the Lyα emission comes from the clumps P_{cl} (p-value 10^{-4}). This does not mean the other parameters do not influence the resulting spectra at all; it means that they cannot be constrained from Tololo 1214-277's observations.

The best values for those parameters that we report here correspond to the values that produce the minimum χ^2. The 1-σ uncertainty comes from a parabolic fit to the χ^2 as a function of $v_{\infty,\text{cl}}$, σ_{cl}, P_{cl} around its corresponding minimum. Under these conditions we find $\sigma_{\text{cl}} = 54.3 \pm 0.6$ km s^{-1}, $v_{\infty,\text{cl}} = 54.3 \pm 5.1$ km s^{-1} and $P_{\text{cl}} = 0.96 \pm 0.01$.

Qualitatively as Tololo 1214-277 possesses a very wide spectrum which can be achieved by subsequent scatterings off (relatively) fast moving clumps while the multi-phase nature (i.e., the existence of low-density channels) ensures the high flux at line center as observed.

DYNAMICAL MASS ESTIMATES

Having constrains for velocity dipersion σ of some dynamical tracers (clumps in the case of the multiphase model) in a spherical system located in a region of size r we estimate the dynamical mass within r.

$$M_{\text{dyn}} = 3\frac{\sigma^2 r}{G} = 3.48\times10^9 \left(\frac{\sigma}{100 \text{ km s}^{-1}}\right)^2 \left(\frac{r}{\text{kpc}}\right) M_\odot \quad (1)$$

As described in the main the letter, we use the 3D half-luminosity radius, r_s, as the typical size for the HI region.

In the case of rotational velocity v in a region of size r we estimate the dynamical mass by

$$M_{\text{dyn}} = \frac{v^2 r}{G} = 1.16 \times 10^9 \left(\frac{v}{100 \text{ km s}^{-1}}\right)^2 \left(\frac{r}{\text{kpc}}\right) M_\odot \quad (2)$$
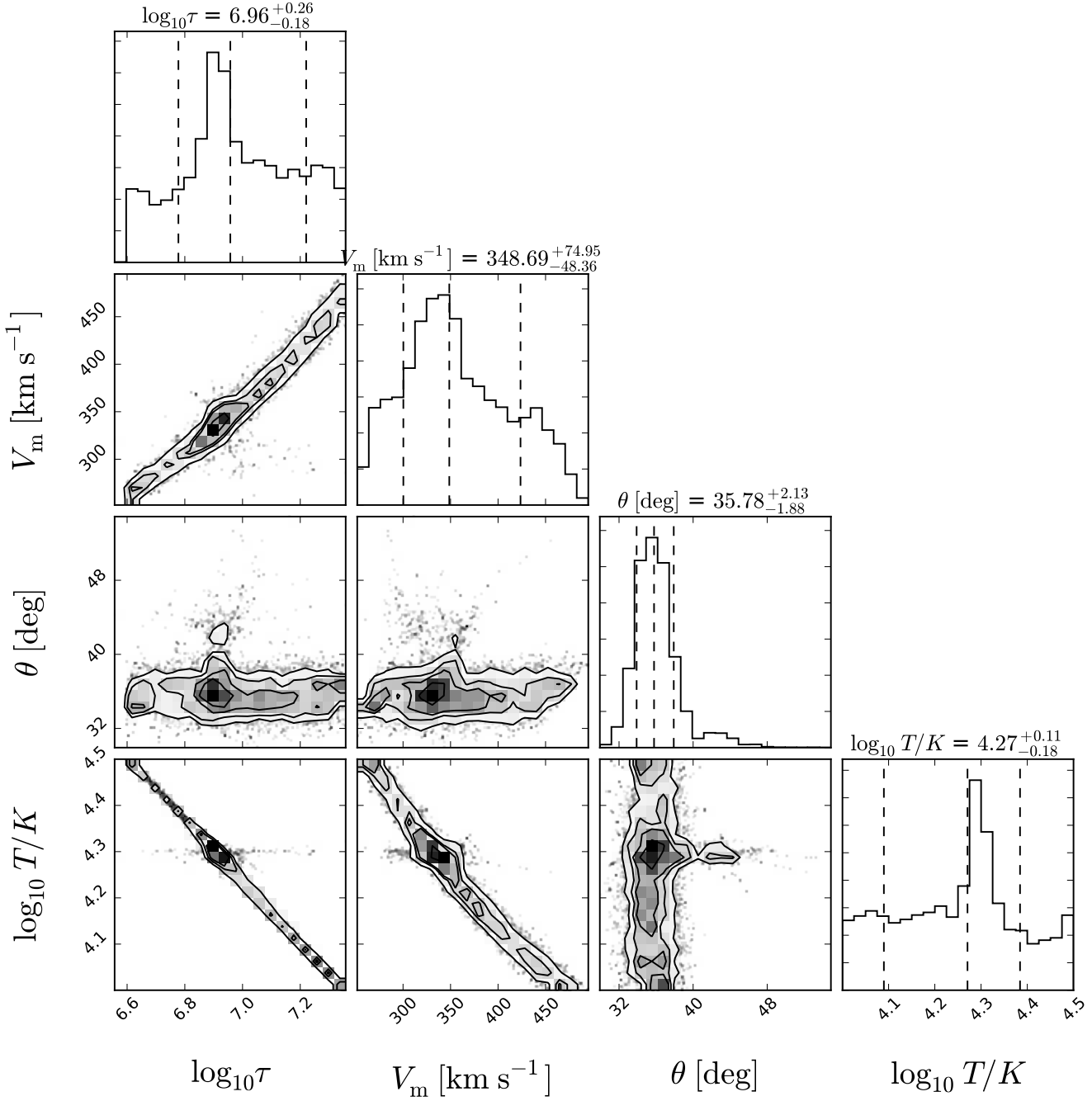
Figure 2. Results from the Markov Chain Monte Carlo computation for the rotation model. The dotted vertical lines in the outer histograms represent the 16th, 50th and 84th percentiles.

REFERENCES

Bacon R. et al., 2014, The Messenger, 157, 13

Dey A., Spinrad H., Stern D., Graham J. R., Chaffee F. H., 1998, ApJL, 498, L93

Dijkstra M., 2014, PASA, 31, e040

Engelbracht C. W., Rieke G. H., Gordon K. D., Smith J.-D. T., Werner M. W., Moustakas J., Willmer C. N. A., Vanzi L., 2008, ApJ, 678, 804

Eskew M., Zaritsky D., Meidt S., 2012, AJ, 143, 139

Foreman-Mackey D., Hogg D. W., Lang D., Goodman J., 2013, PASP, 125, 306

Forero-Romero J. E., Yepes G., Gottlöber S., Knollmann S. R., Cuesta A. J., Prada F., 2011, MNRAS, 415, 3666

Garavito-Camargo J. N., Forero-Romero J. E., Dijkstra M., 2014, ApJ, 795, 120

Graves G. J., Faber S. M., Schiavon R. P., 2009, ApJ, 698, 1590

Gronke M., Bull P., Dijkstra M., 2015, ApJ, 812, 123

Gronke M., Dijkstra M., 2014, MNRAS, 444, 1095

Gronke M., Dijkstra M., 2016, ApJ, accepted

Hummer D. G., Storey P. J., 1987, MNRAS, 224, 801
Izotov Y. I., Papaderos P., Guseva N. G., Fricke K. J., Thuan T. X., 2004, A&A, 421, 539
Laursen P., Duval F., Östlin G., 2013, ApJ, 766, 124
Madden S. C. et al., 2014, PASP, 126, 1079
Noeske K. G., Papaderos P., Cairós L. M., Fricke K. J., 2003, A&A, 410, 481
Östlin G. et al., 2014, ApJ, 797, 11
Partridge R. B., Peebles P. J. E., 1967, ApJ, 147, 868
Pustilnik S. A., Martin J.-M., 2007, A&A, 464, 859
Rivera-Thorsen T. E. et al., 2015, ApJ, 805, 14
Seth A. C. et al., 2014, Nature, 513, 398
Thuan T. X., Izotov Y. I., 1997, ApJ, 489, 623
Tollerud E. J., Bullock J. S., Graves G. J., Wolf J., 2011, ApJ, 726, 108
Verhamme A., Schaerer D., Maselli A., 2006, A&A, 460, 397